scientific reports

Check for updates

OPEN

Microglial depletion prevents visual deficits and retinal ganglion cell loss induced by early life stress in adult animals

Juan S. Calanni[1], Laura A. Pasquini[2], Hernán H. Dieguez[3], Nathaly Bernal Aguirre[3], Bruno G. Berardino[4], Damian Dorfman[3] & Ruth E. Rosenstein[1]✉

Early life stress (ELS), a prenatal/early postnatal period of severe trauma, social deprivation, or neglect, among other adversities, constitutes a risk factor for developing psychopathologies and different health complications in adulthood. Maternal separation with early weaning (MSEW) induces long-term consequences in mouse retinal function and structure. We analyzed microglia involvement in adult retina ELS-induced sequelae. C57Bl/6 J mice were separated from the dams at postnatal days (PND) 4–6, 7–9, 10–12, and 13–16, for 2 h, 3 h, 4 h, and 6 h, respectively, and were weaned at PND 17. Control pups were left undisturbed and weaned at PND 21. At PND 45, MSEW induced microgliosis and decreased retinal ganglion cell (RGC) function, followed by RGC loss at PND 60. Microglial phenotypic alterations correlated with a pro-inflammatory profile (i.e., increase in the nuclear levels of nuclear factor kappa B -subunit p65, and C3-, nitric oxide synthase-2, and interleukin-1β-immunoreactivity in Iba-1 (+) cells). Depleting microglia between PND 35 and 60 did not affect the retina from naïve mice. However, in early stressed mice, it preserved RGC function and number, visually mediated behavior, and contrast sensitivity. Therefore, microglial reactivity could be one of the key factors linking progressive alterations provoked by ELS in adult mice retinal function and structure.

Keywords Early life stress, Retina, Visual functions, Microglia, Retinal ganglion cells, Microglia depletion

Early life stress (ELS) refers to a prenatal/early postnatal period of severe and/or chronic trauma, environmental/social deprivation, neglect, or abuse, among other adversities[1,2]. Exposure to adversities during childhood is a risk factor for developing psychopathologies and other health complications later in life. In fact, depression, substance abuse, panic attacks, anxiety, social phobia, and suicidal behavior, as well as cardiovascular and respiratory diseases, diabetes, obesity, and cancer have been strongly associated with ELS[3–9]. It has been estimated that 22—32% of adult psychopathology may be attributed to a history of early life adversity[10].

During childhood, social ties (mother-infant in particular), have a critical role in brain development and adult behavior. In this line, maternal separation (MS), dramatically affects brain development and augments the risk for different diseases in adulthood[11–13]. Studies in rodents have reported that pup separation from their dams during early life increases long-lasting depressive-like and/or anxiety-like behaviors in adulthood[12,13]. Moreover, animal studies have demonstrated ELS-induced neural and behavioral deficits that persist throughout the lifespan[11,14]. MS with early weaning (MSEW) in mice involves separating pups from the dam for extended periods across repeated days during the pre-weaning period (i.e., when offspring are highly dependent on maternal care), and weaning at PND 17 (i.e., 4 days ahead of control mice). MSEW mimics early life maternal neglect and is recognized as an adequate preclinical model to emulate early adverse experiences. MSEW shows

[1]Laboratory of Retinal Neurochemistry and Experimental Ophthalmology, Department of Biological Chemistry/IQUIBICEN, School of Science, University of Buenos Aires/CONICET, Ciudad Autónoma de Buenos Aires (C1428EHA) Argentina, Av. Int. Güiraldes 2620, Pabellón II, 2º Piso, Ciudad Autónoma de Buenos Aires, Argentina. [2]Department of Biological Chemistry and Institute of Chemistry and Biological Physicochemistry, IQUIFIB, School of Pharmacy and Biochemistry, University of Buenos Aires/CONICET, Ciudad Autónoma de Buenos Aires, Argentina. [3]Laboratory of Retinal Neurochemistry and Experimental Ophthalmology, Department of Human Biochemistry, School of Medicine/CEFYBO, University of Buenos Aires/CONICET, Ciudad Autónoma de Buenos Aires, Argentina. [4]Neuroepigenetics Laboratory, Department of Biological Chemistry/IQUIBICEN, School of Science, University of Buenos Aires/CONICET, Ciudad Autónoma de Buenos Aires, Argentina. ✉email: ruthr@fmed.uba.ar

behavioral deficits like those observed in neglected humans, such as hyperactivity, anxiety and attentional deficits[3,15–17].

ELS long-term consequences seem to be related to alterations in brain regions, such as the hippocampus, the prefrontal cortex, and the amygdala characterized by plasticity and delayed developmental processes[18–20]. Reduced gray matter in the left hemisphere primary visual cortex has been found in studies comprising young adults with a history of childhood sexual abuse or witnessed domestic violence, and children diagnosed with reactive attachment disorder and exposed to various types of maltreatment[21–23]. There is some evidence of the effects of childhood maltreatment in brain regions controlling primary sensory cortices, but very few studies have explored the respective sensory organs connected to these brain regions[23]. In fact, although the retina is part of the central nervous system, ELS sequelae in the adult retina have received, so far, little attention. In this context, we have recently demonstrated that MSEW decreases retinal ganglion cell (RGC) function and induces an impairment of the performance in visually-guided behavioral tests, along with inner (but not outer) retinal microgliosis, followed by RGC loss in adult male and female C57Bl/6 J mice[24].

Some studies have shown that stress-induced alterations are not only associated with neuronal function, but also have a significant impact on glial cells including microglia, astrocytes, and oligodendrocytes[20,25,26]. Grigoruta and collaborators[27] have studied the effect of MS in the retina of female *Wistar* rats. In this study, newborn pups were separated from their mother from day 2 to 14 for 3 h a day. An increase in retinal microglial markers were observed in adolescent, adult, and aged MS animals[27], while the gliotic marker glial fibrillary acidic protein (GFAP), was only observed in old mice submitted to ELS. Glial cells are essential players in normal neuronal function; thus, their alterations may lead to significant impairments[28]. For this reason, investigating how stressful events during vulnerable periods of life can modify glial cells may contribute to understanding the basis of ELS sequelae. Despite the fact that results from rodent studies have been conflicting, one potential mechanism associated with ELS sequelae is the disruption of microglial cell density and morphology[20]. In this context, the aim of this work was to analyze the involvement of microglial cells on visual alterations induced by MSEW. In addition, the consequences of microglial depletion in the functional and structural sequelae induced by MSEW in the adult retina were analyzed. BLZ945, a specific inhibitor of colony stimulating factor 1 receptor (CSF1R) that induce microglial depletion was administered. CSF1R is a key signaling node in microglia and macrophage biology. In fact, CSF1R signaling is not only required for the proper development of these cell populations but is also a critical regulator of their homeostasis in adulthood[29]. In particular, CSF1R signaling modulates proliferation, migration, differentiation, and survival of microglia and macrophages in health and disease[30,31].

Results

Temporal course of the retinal function in control or MSEW animals

Figure 1 depicts scotopic ERGs recorded at postnatal day (PND) 35, 45 and 60 in control or MSEW mice. No significant differences in ERG a- and b-wave amplitudes were observed between groups throughout the study. However, at PND 45, positive scotopic threshold response (pSTR) and photopic negative response (PhNR) amplitudes (i.e., both indexes of RGC function) significantly decreased in MSEW animals (10.02% and 15.09% compared to control, respectively). A further decrease of these parameters (30.84% and 32.39% compared to control, respectively) was observed at PND 60. Representative ERG recordings from control and MSEW mice are also shown in Fig. 1.

Effect of MSEW on retinal microglial activation

In order to study microglial activation at PND 35, 45 and 60, two morphometric analyses were performed: Sholl analysis that evaluates the complexity and branching of the processes, and cell circularity, which is an index of the range from ramified to ameboid cells. At PND 35, there was no significant change in branching complexity between both groups. However, at PND 45, a significant reduction of the area under the curve in the MSEW group as compared with controls was observed, suggesting a decrease in microglial ramification at this stage. This difference significantly increased at PND 60. Regarding cell circularity, 100% of cells in both groups exhibited circularity values ranging from 0 to 0.1. At PND 45, the proportion of cells within that circularity range decreased to approximately 70%, accompanied by a shift towards higher circularity values, indicative of a greater presence of ameboid microglial cells in early stressed mice. This trend was further accentuated by PND 60, with the proportion of cells within the circularity range from 0 to 0.1 declining to around 50% (i.e., showing greater values than 0.1), indicating an even greater presence of ameboid profile within microglial population (Fig. 2). At PND 60, the levels of GFAP—a gliotic marker predominantly expressed by damaged Müller cells in the retina—did not differ between control and MSEW mice (see Supplementary Figure S1).

At PND 45, MSEW induced an increase in the nuclear levels of nuclear factor kappa B (NFkB) subunit p65, as well as in C3-, nitric oxide synthase-2 (NOS-2)-, and interleukin-1β (IL-1β)-immunoreactivity within Iba-1-(+) cells (Fig. 3).

Effect of MSEW on RGC number

The temporal course of Brn3a (+) RGC number in flat-mounted retinas is shown in Fig. 4.

MSEW did not affect this parameter both at PND 35 and PND 45, whereas a significant decrease in Brn3a (+) RGC number was observed at PND 60.

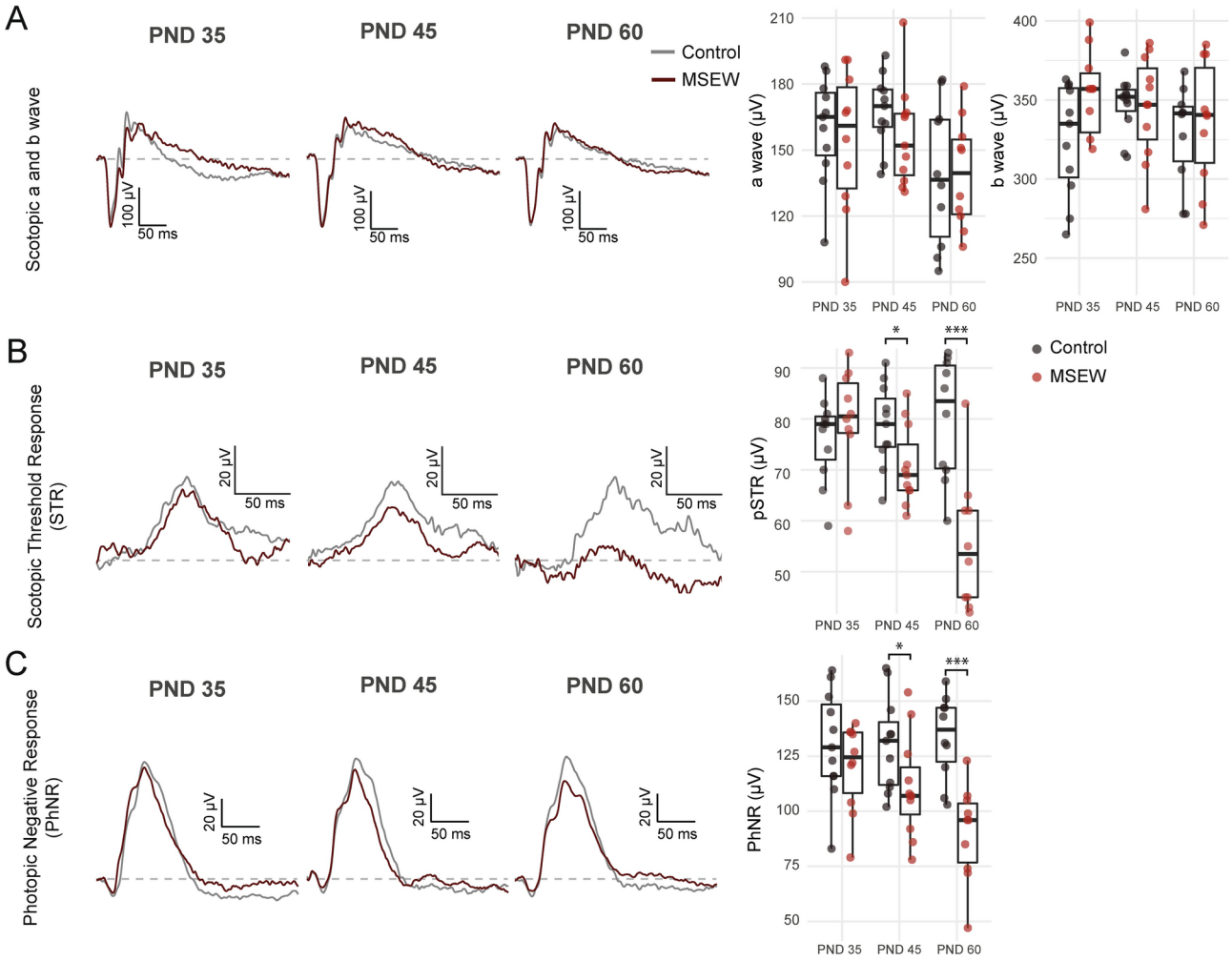

Fig. 1. Temporal course of the retinal function in control or MSEW animals. **A**. Scotopic ERG a-wave and b-wave amplitudes. No changes in these parameters were observed throughout the study. **B**. pSTR amplitude, and **C**. PhNR amplitude at PND 35, 45 and 60. pSTR and PhNR amplitude significantly decreased in MSEW mice at PND 45 and further diminished at PND 60. Representative scotopic ERG, pSTR and PhNR traces from control and MSEW animals are shown in the left margin of each panel. ANOVA and Tukey post hoc tests were conducted. Significance levels: *P < 0.05, *** P < 0.001, n = 10–11 litters/group.

Effect of microglia depletion on retinal function, RGC number and vision-guided behavior in control mice

In control mice, BLZ945 administration from PND 35 to PND 60 depleted retinal microglial cells but did not affect scotopic ERG a-wave and b-wave amplitudes, as well as RGC function (pSTR and PhNR amplitudes) and Brn3a (+) RGC number (Fig. 5).

In addition, BLZ945 did not affect general locomotor activity or visual function (measured by the looming test with contrast variation (LTCV)) (Fig. 6).

Effect of microglia depletion in MSEW mice

In MSEW mice, BLZ945 depleted Iba-1 (+) cells, improved RGC function (22.35% and 16.51% for pSTR and PhNR amplitudes, respectively, compared to vehicle-treated MSEW animals), and preserved Brn3a (+) RGC number, without changing scotopic ERG a-wave and b-wave amplitudes, compared to MSEW animals that received vehicle. Moreover, MSEW animals treated with BLZ945, which did not affect general locomotor activity before looming stimulus application, showed a better performance in the LTCV, which correlated with a significant decrease in the C50 (Fig. 7).

Discussion

The present results indicate that MSEW provoked progressive retinal alterations and that microglial activation could be one of the key factors linking the long-term consequences in retinal function and structure with MSEW. It has been clearly demonstrated that ELS increases the vulnerability to psychopathologies later in life; however, neurobiological mechanisms underlying the emergence of these changes have been poorly characterized.

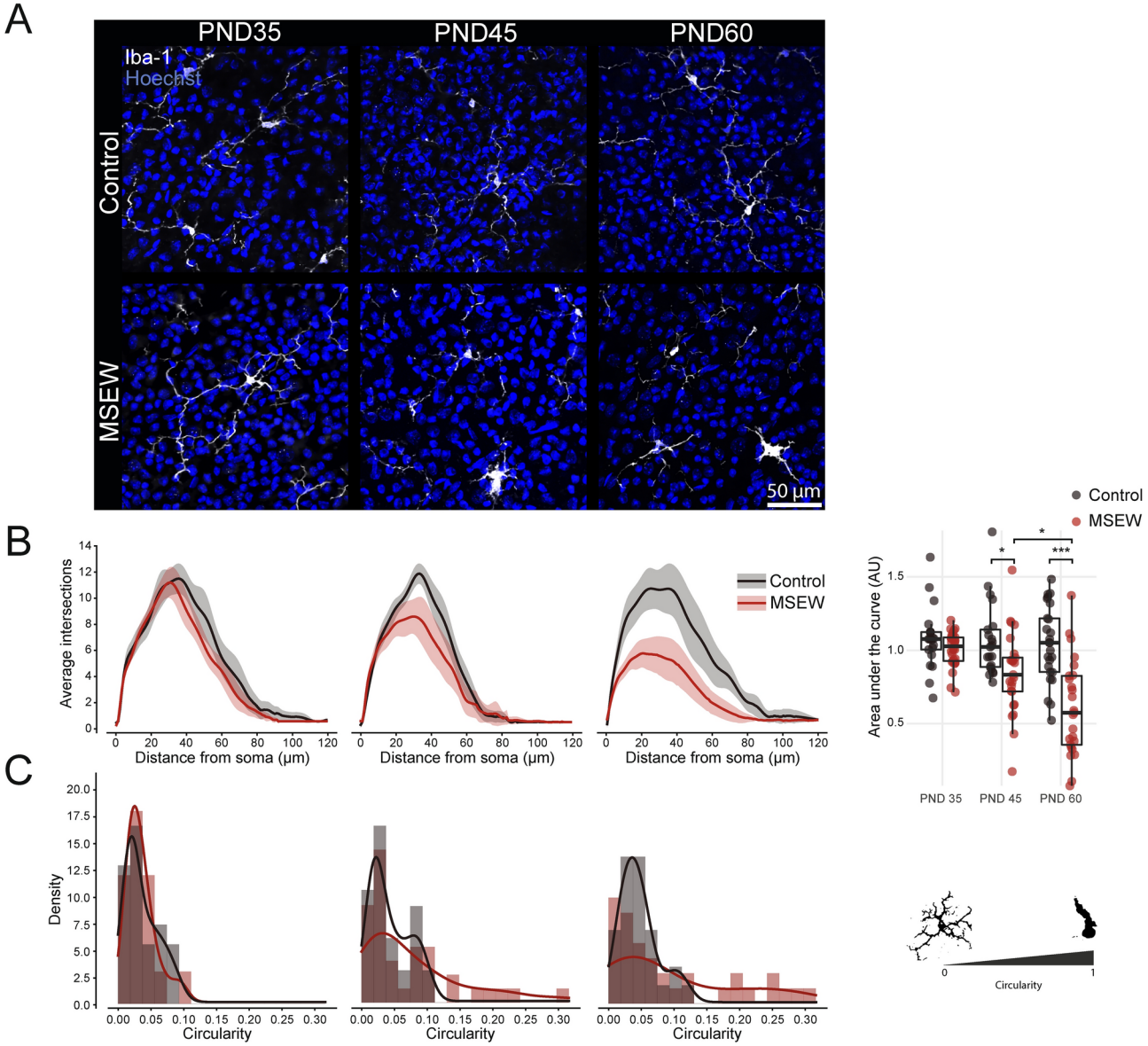

Fig. 2. Effect of MSEW on microglial morphology. **A**. Representative confocal micrographs of Iba-1-immunostaining in flat mounted retinas. **B**. Sholl analysis of microglia within the inner retina, which revealed no significant alterations in branching complexity at PND 35, but a significant reduction in the area under the curve at PND 45 in the MSEW group as compared to controls. **C**. Distribution density for microglial circularity at GCL layer. At PND35, 100% of cells exhibited circularity values range from 0 to 0.1 in both groups. In the MSEW group, the proportion of cells within this circularity range (i.e., 0 to 0.1) decreased to approximately 70%, accompanied by a higher circularity range value. At PND 60, this trend was further accentuated, declining to around 50% the proportion of cells within the 0 to 0.1 circularity range. ANOVA and Tukey post hoc tests were conducted. Significance levels: *P < 0.05, ***P < 0.001, n = 6–7 litters/group (a range of 6 to 8 cells was analyzed).

Notwithstanding, emerging evidence indicates that microglial cells, the specialized resident macrophages of the brain, are implicated in the development of ELS sequelae[20,32–34], such that microglia may be a central cellular mediator of the relationship between early stressor exposure and neuropsychiatric disorders in adulthood. In adult animals, a meta-analysis supports evidence that ELS induces a stronger increase in microglia density and soma size, without changes in astrocytes[20]. Moreover, some studies have associated ELS-induced impairments with a chronic inflammatory state, which could be provoked by microglial reactivity[34,35]. Regarding the retina, MSEW induced a progressive decline in RGC function, as evidenced by decreased pSTR and PhNR amplitudes, which was evident at PND 45 (but not at PND 35), and worsened by PND 60. No alterations in outer retinal function were observed throughout the study (i.e., scotopic ERG a- and b-wave amplitudes). Contrasting our findings, a decrease in the outer nuclear layer thickness in adolescent rats submitted to MS has been described[27]. Currently, we have no explanation for this discrepancy; however, differences in species, protocols used for

MS, methodological variations in imaging techniques, developmental stages analyzed, or markers used could account for it.

To get insight into microglial involvement in visual ELS-induced progressing sequelae, the temporal course of retinal microglia morphology within MSEW was also analyzed. For this purpose, two morphometric analyses were performed: Sholl index, which evaluates both the complexity of microglial branching and the territory they occupy, and cellular circularity. Microglial morphology remained unchanged at PND 35 in early stressed mice, whereas at PND 45, Sholl analysis demonstrated a reduced area under the curve in plots representing intersections against distance from the inner retinal soma from MSEW animals, indicating a reduced branching complexity. In agreement, cellular circularity analysis showed activated microglia that displayed reduced length, thicker processes, and larger cell somas or no processes (amoeboid) in retinas from MSEW mice, compared to resting microglia (which are small-bodied and highly ramified) in control mice. The reactive microglial profile became more pronounced at PND 60, aligning with the hypothesis of a gradual escalation in the retinal microglia phenotype from MSEW animals. In agreement, in female *Wistar* rats submitted to MS, an increase in retinal microglial markers is observed[27].

At PND 45, microglial phenotypic alterations correlated with a pro-inflammatory profile and RGC dysfunction (i.e., decreased pSTR and PhNR amplitudes). At PND 60, MSEW further increased RGC dysfunction, decreased the performance in a vision-guided behavioral test[24], and induced RGC loss. Of note, MSEW that does not affect the outer retinal microglia[24], did not change the outer retinal function, which could be considered as indirect evidence that microglial role in adult animals submitted to MSEW could be region-dependent within the retina.

Several reports indicate that ELS disrupts microglial function[33]. However, other studies suggest a resilience mechanism in these cells. Exposure to a single stressful event may not be enough to induce significant long-term alterations. Instead, ELS may prime microglial cells, enhancing their reactivity or vulnerability to subsequent challenges, which could eventually lead to long-term functional impairments. This phenomenon, recognized as the "double-hit hypothesis" indicates that an initial early adverse event may prime microglial response to a second negative challenge[36–38]. In contrast, in our experimental setting, MSEW per se induced a reactive phenotype in retinal microglia, even in the absence of a subsequent challenge.

It has been described that ELS induces sex-specific changes on several parameters in adult animals[39,40]. Although in mice subjected to MS from PND 2 to 14 there is an increase in microglial soma size in the hippocampus from females, but not from males at PND 42[41], no sex-dependency was observed in MSEW-induced retinal microglial changes. Studies on microglial morphophysiological heterogeneity have demonstrated correlations between microglial morphometric parameters and IL-1β expression levels, suggesting that the degree of microglial activation cannot be solely characterized by structural changes from ramified to ameboid shapes[42].

To assess whether microglial morphological changes reflect a shift to a pro-inflammatory functional state, inflammatory signals were assessed at PND 45. The variation in microglial morphology was consistent with an increased expression of pro-inflammatory signals localized within Iba-1 (+) cells. In this context, nuclear translocation of NFkB p65 subunit, as well as C3-, NOS-2-, and IL-1β-immunoreactivity significantly increased in inner retinal Iba-1 (+) cells from MSEW-exposed mice. In contrast, no changes in NFkB levels were described in the retina from old rats submitted to MS[27]. The activation of NFkB in microglia is critically associated with retinal detrimental effects within several pathological conditions, such as diabetic retinopathy, excitotoxicity, and optic nerve crush, among others[43–46]. Thus, dysregulated inflammatory responses involving microglial activation, including complement C3 deposits may be involved in retinal dysfunction and RGC loss induced by MSEW. The retinal expression of C3 has been attributed to astrocytes[47]and retinal pigment epithelium cells[48]. However, in non-physiological conditions, such as experimental retinitis pigmentosa (RP, the rd10 retina), human specimens of RP, retinal damage induced by N-methyl-D-aspartate[49], light-induced photoreceptor injury[50], and in the retina from leptin-deficient (ob/ob) mice[51], activated microglia comprises the main source of C3. C3 deficiency decreases microglial phagocytosis[52]. Since MSEW induces RGC phagocytosis by microglia[24], a microglial C3-mediated phagocytosis pathway could be involved in RGC loss induced by ELS, although the involvement of other mechanisms cannot be ruled out. Studies are in progress to analyze this issue. In any case, since microglial cell alterations preceded changes in RGC number that were evident at PND 60 (but not before), it seems possible that microglial activation may play a causal role in MSEW-induced RGC loss, and consequently in visual function alterations in adulthood. As a proof of concept for this hypothesis, microglia from control or MSEW mice were pharmacologically depleted from PND 35 to PND 60. Minocycline has been widely used in the past (and still is) to demonstrate microglial involvement, thanks to its favorable kinetic properties and its relatively low cost. In this line, it has been demonstrated that ELS induces alterations in dopaminergic neuron morphology, reduces dopamine transporter and tyrosine hydroxylase expression that are prevented by minocycline[53], which also avoids early axoglial alterations of the optic nerve in an experimental model of glaucoma[54]. However, minocycline has low specificity (i.e., effects on other immune cells, subtle effects on astroglial activation, controversial mechanism of action, and possible effects on microbiota); thus, more specific tools should be considered. The CSF1R antagonist, PLX3397, has been used to investigate the effects of retinal microglia depletion and repopulation; however, contradictory results were obtained with its use in different experimental settings. For example, it has been shown that after PLX3397 withdrawal, microglial repopulation attenuates pathological choroid neovascularization and dampened cellular senescence in a model of exudative age-related macular degeneration[55], and significantly improves the retinal outer nuclear layer structure, the electroretinographic response, and the visual behavior in rd10 mice[56]. Laudenberg and collaborators[57] demonstrated that microglia depletion by PLX3397 decreases the expression of several key pro-inflammatory factors, but is unable to influence the extent of retinal degeneration in a mouse model of light-induced retinal degeneration. Furthermore, Karg et al.[58] showed that aged C57Bl/6 mice fed for 6 weeks with chows containing PLX5622 that efficiently depleted retinal microglia, show a significant loss in visual function, presenting reduced

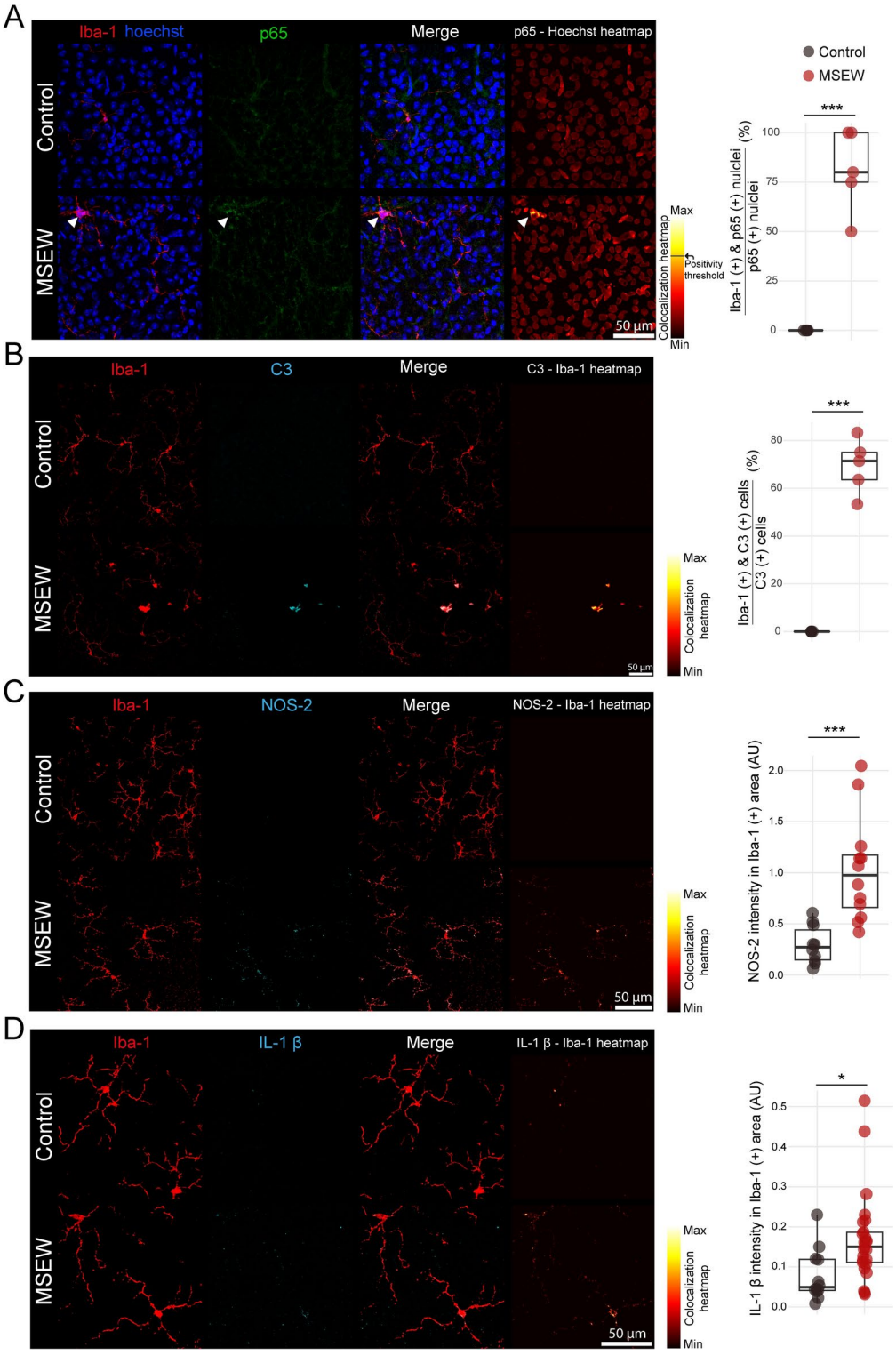

contrast sensitivity, and impaired retinal pigment epithelium function. Microglia depletion with either PLX3397 or PLX5622 causes functional impairment of rods and cones in a rat model of RP[59]. Based on the conflicting results with PLX3397 and PLX5622, the effect of another CSF1R antagonist (BLZ945), which has not been tested at the level of retinal microglia, was analyzed. As shown herein, microglial cell depletion by BLZ945 treatment from PND 35 to PND 60 did not affect per se neither outer and inner retinal function (ERG a-wave, b-wave, pSTR and PhNR amplitudes), nor RGC number in naïve mice. The electrical response to a light flash (ERG) provides a reliable information about the retinal function; however, vision is a much more complex and integral function. Recently, based on the rodent innate response to the looming stimulus, we have developed a new test by varying disk/background contrast (i.e., the LTCV) that provides a quantitative measurement, the C50, which can be used as an index of contrast-sensitivity[60]. Therefore, we analyzed the effect of microglia depletion on the performance of control mice in the LTCV. BLZ945 treatment did not affect locomotor activity assessed

◂**Fig. 3**. MSEW increased inflammatory marker levels in microglia at PND 45. Representative confocal micrographs of Iba-1-immunostaining in flat mounted retinas. **A**. Colocalization heatmap showing NFkB p65 subunit immunofluorescence intensity in Hoechst(+) nuclei. A positivity threshold was arbitrarily chosen to classify nuclei as positive or negative for NFkB p65 subunit. White arrow shows nuclei above positivity threshold from a Iba-1 (+) cell. Right panel: Quantification of the percentage of nuclei NFkB p65(+) in Iba-1 (+) cells is shown. B. Colocalization heatmap showing C3-immunoreactivity in Iba-1 (+) area. Right panel: Quantification of the percentage of C3(+) cells which are also Iba-1 (+). C. Colocalization heatmap showing NOS-2-immunoreactivity in Iba-1 (+) cells. Right panel: Quantification of NOS-2 immunoreactivity in Iba-1 (+) cells. D. Colocalization heatmap showing IL-1β-immunofluorescence intensity in Iba-1 (+) cells. IL-1β intensity within Iba-1 (+) area was quantified (right panel). The colocalization of Iba-1 with C3- (**B**), NOS-2- (**C**), and IL-1β-immunoreactivity (**D**) was significantly higher in retinas from MSEW than control mice. For NOS-2 and IL-1β, a range of 6 to 8 Iba-1 (+) cells in each retina was analyzed, n = 5 litters/group. ANOVA and Tukey post hoc tests were conducted. Significance levels: *P < 0.05, ***P < 0.001.

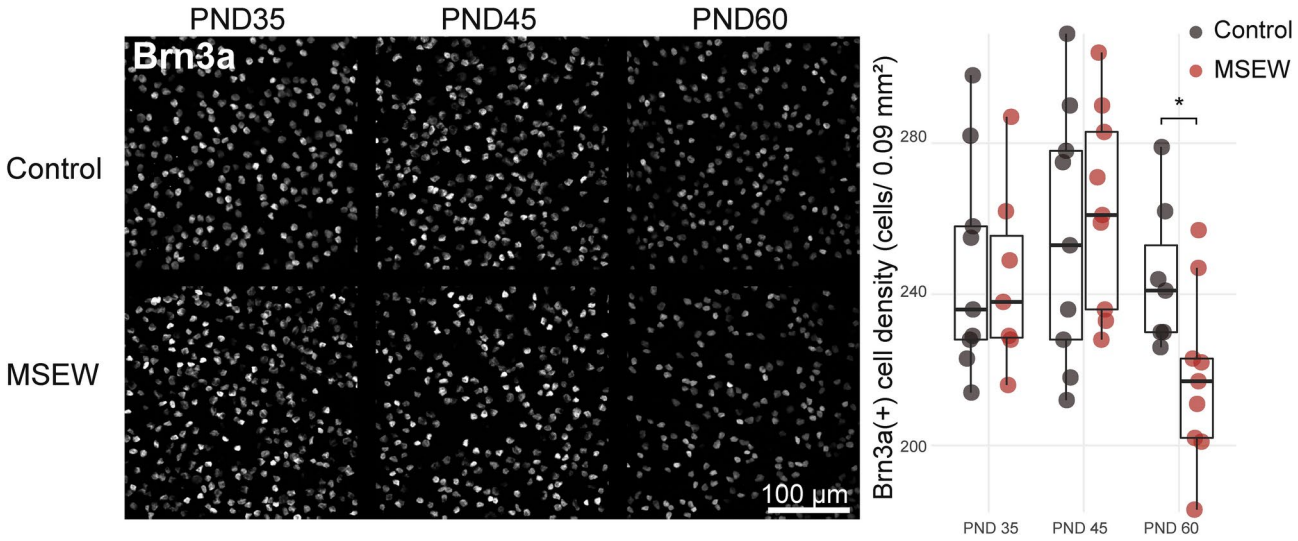

Fig. 4. Effect of MSEW on RGC number. Representative confocal micrographs of Brn3a-immunostaining in flat-mounted retinas. MSEW did not affect this parameter at PND 35 and 45, whereas at PND 60, a significant decrease in Brn3a-(+) RGC number was observed. ANOVA and Tukey post hoc tests were conducted. Significance levels: *P < 0.05, n = 7–9 litters/group.

before stimulus application. Additionally, it did not alter contrast sensitivity in the LTCV test, consistent with the lack of effect on RGC number. In contrast, when MSEW animals were treated with BLZ945 from PND 35 to PND 60, an improvement in RGC function and preservation of their number were evident, without affecting the outer retinal function. Notwithstanding, a limitation of this study lies in the use of Brn3a to assess RGC number, which may underestimate this parameter, as it does not label all RGC subtypes. Microglia depletion with BLZ945 treatment improved contrast-sensitivity in the LTCV, as shown by a decrease in the C50 within adult mice submitted to MSEW.

Working with humans exposed to ELS is limited by the difficulties of finding a statistically useful sample of individuals that have undergone early adversities at the same stage, duration, and intensity. In contrast, using animal models allows controlling the stress duration and type, as well as the developmental stage at which stressful events occur[59,60]. Notwithstanding, findings showing MSEW effects in the mouse adult retina are consistent with the recent demonstration that the retinal nerve fiber layer (RNFL) and the ganglion cell layer (GCL), along with the inner plexiform layer of the macula were significantly thinner in both eyes from children and adolescents aged 9–18 submitted to early maltreatment experiences, whereas no significant differences in other retinal regions or microvasculature were observed in humans submitted to childhood maltreatment[23]. More recently, in the largest pediatric neuroimaging data sets yet across eight contributing sites in four countries, focused from birth to 6 years of age, it has been shown that several forms of ELS, such as preterm birth, low birthweight, low maternal education, and low family income, significantly decrease visual reception scores[61].

Conclusions: Taken together, these results suggest that even in humans, ELS-induced visual alterations in adults should be considered among the threats to life quality resulting from childhood adversities. Although total or partial microglial depletion could compromise retinal defense against future adverse events, immune surveillance, functional support, and maintaining homeostasis, our results suggest that modulating microglial reactivity may be a novel strategy to avoid ELS-induced visual alterations.

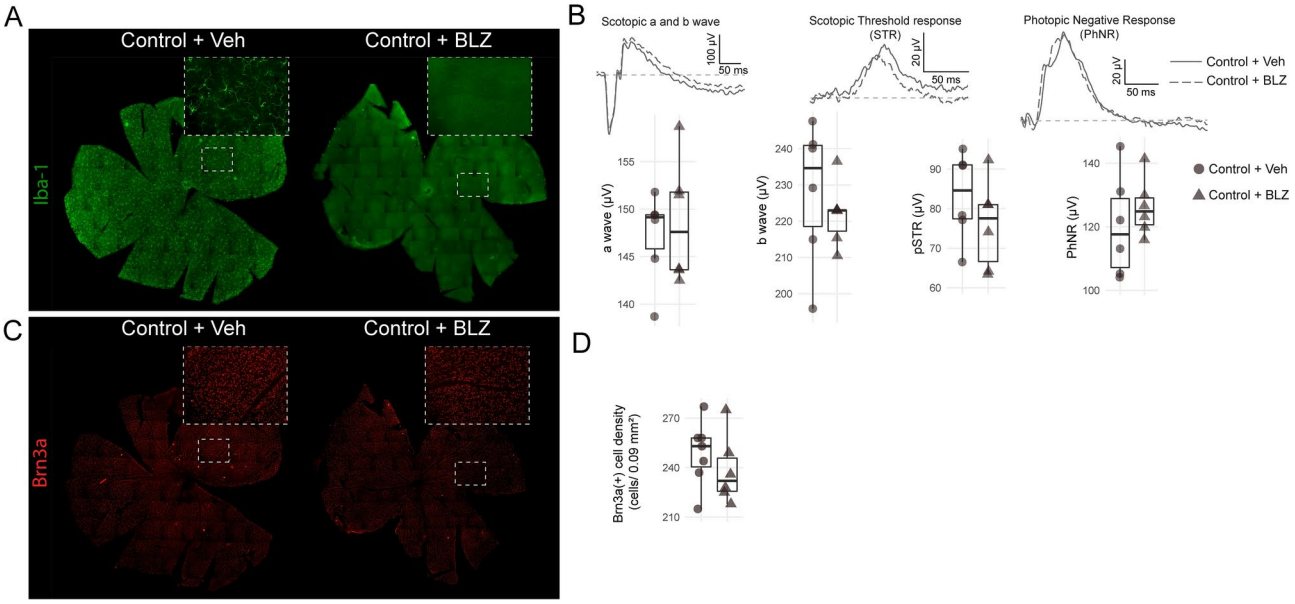

Fig. 5. Effect of BLZ945 treatment from PND35 to PND60 in control mice. **A**. Representative images of Iba-1-immunoreactivity in the inner retina. BLZ945 depleted retinal microglial cells. **B**. BLZ945 did not affect ERG a-wave, b-wave, pSTR and PhNR amplitudes. **C**. Representative images of Brn3a-immunoreactivity. **D**. BLZ945 did not affect Brn3a (+) RGC number. ANOVA and Tukey post hoc tests were conducted, n = 6–7 litters/group.

Materials and methods

Animals

Male and female C57Bl/6 J mice (Research Resource Identifiers (RRID):IMSR_JAX:000,664) were obtained from the bioterium of the School of Pharmacy and Biochemistry, University of Buenos Aires, and were bred in house and kept under controlled temperature, luminosity, and humidity, and a 12-h light/12-h dark period (lights on at 8:00 AM). When needed for experimental procedures, animals were anesthetized with intraperitoneal injection of 110 mg/kg ketamine hydrochloride and 10 mg/kg xylazine hydrochloride. Euthanasia was performed by CO_2 asphyxiation, followed by cervical dislocation. All procedures were in strict accordance with the Research Reporting of In-Vivo Experiments (ARRIVE) guidelines, and in accordance with the National Research Council´s Guide for the Care and Use of Laboratory Animals. The ethics committee of the School of Medicine, University of Buenos Aires (Institutional Committee for the Care and Use of Laboratory Animals, (CICUAL)) approved this study, and all efforts were made to minimize animal suffering. Experimental groups included male and female mice because in a previous report we showed that retinal parameters of function and structure did not differ between sexes[24]. The numbers of male and female mice were balanced across the experimental groups.

Study design

A validated mouse model of ELS (i.e., MSEW) was used as previously[24] For this purpose, pregnant females were randomly assigned to control or MSEW groups at (PND) 0. At PND 3, all litters were culled to 6 animals (3 males and 3 females). Litters with less than 6 animals were discarded. From PND 4 to PND 16, mothers from the MSEW group were removed from their cages at 12:00 p.m. every day and placed in a clean cage with ad libitum access to food and water. Separation times were: 2 h at PND 4–6, 3 h at PND 7–9, 4 h at PND 10–12, and 6 h at PND 13–16. At the end of each separation period, mothers were subjected to a movement restriction protocol in an opaque polyvinyl chloride tube (15 cm long × 4.5 cm diameter) for 10 min, and then returned to the cage. Finally, MSEW pups were weaned at PND 17, as shown in Fig. 8. Control pups were weaned at PND 21 and were only disturbed for cage cleaning and weight measurement, which did not differ from MSEW mice throughout the study (data not shown). At PND 27, animals from different litters were identified, and relocated in female/male only cages, containing 4 animals each. Each litter was considered an experimental unit. To analyze the evolution of retinal changes over time, animals from different litters were collected for functional studies and tissue harvesting. To analyze the effect of microglia depletion, one group of animals received 200 mg/kg BLZ945 (Sotuletinib, a potent, selective and brain-penetrant colony stimulating factor 1 receptor) or vehicle (0.5% methylcellulose), once a day, by oral gavage from PND 35 to PND 60 (Fig. 8). BLZ945 was kindly provided by Novartis, Basel, Switzerland, and its administration way and dosage were selected based on a previous report[62]. No animals were excluded from the experiments. Different animals within the litters were used for functional tests or tissue harvesting.

Electroretinography

Electroretinographic activity was assessed using mice from different litters, as previously described[24,63]. Briefly, after 12 h of dark adaptation, mice were anesthetized under dim red illumination. Phenylephrine hydrochloride

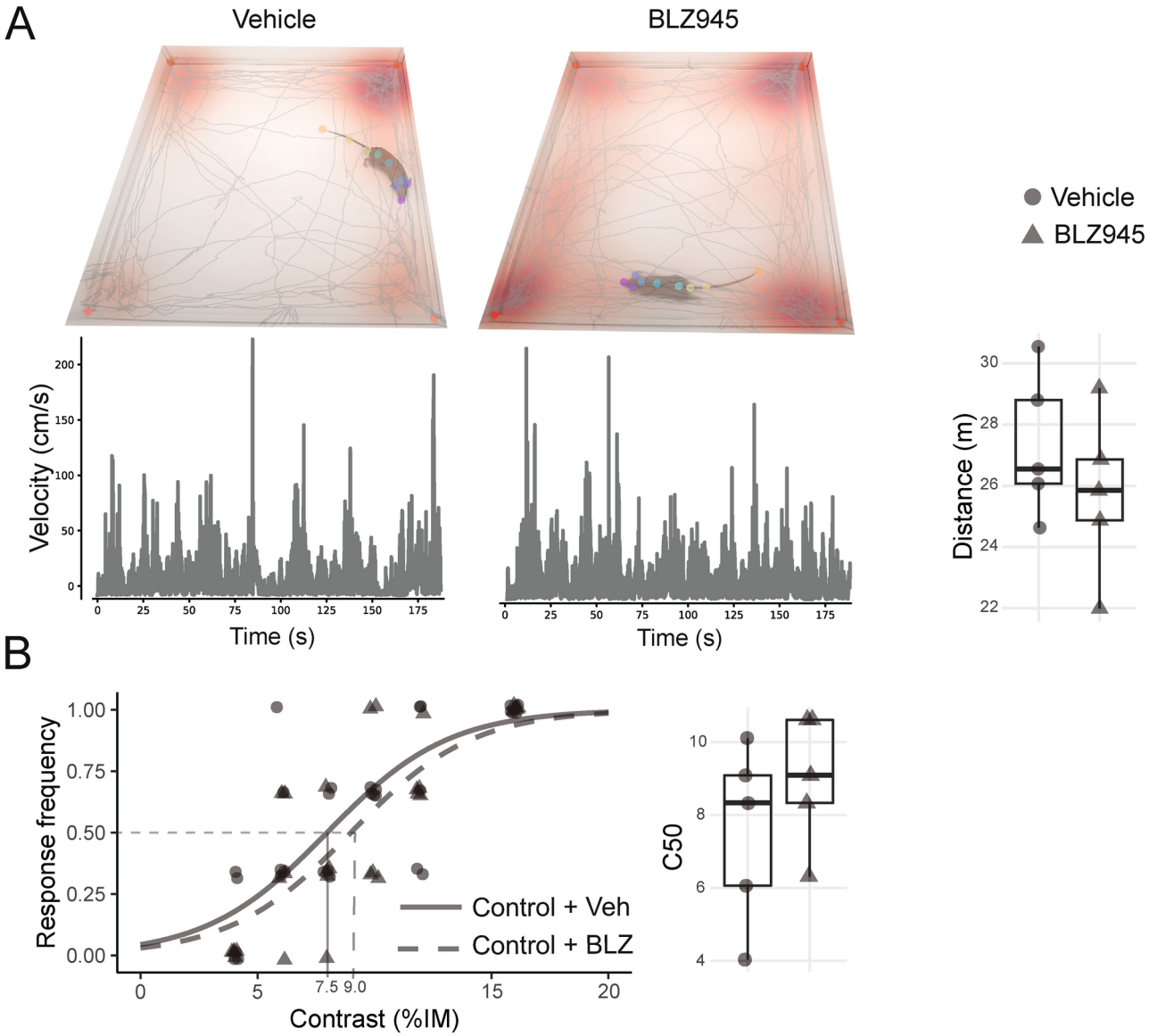

Fig. 6. Effect of microglial depletion on a vision-guided behavioral test in control mice. **A**. Representative mouse tracking and velocity assessment during pre-stimulus exploratory period. BLZ945 did not affect exploratory behavior nor locomotor activity, as shown by the distance covered during exploration. **B**. BLZ945 did not affect control mouse performance in the LTCV test nor the C50. ANOVA and Tukey post hoc tests were conducted, n = 5 litters/group.

and tropicamide were used for pupil dilatation, and the cornea was intermittently irrigated with balanced saline solution to prevent keratopathy and maintain the baseline recording. Electroretinograms (ERG) were recorded with a HMsERG model 2000 (Ocuscience LLC, Kansas City, MO, USA), equipped with a Ganzfield dome fitted with a white light emitting diode stimulus at 2 cm from the eye. A reference electrode was placed through the ear, a grounding electrode was attached to the tail, and a silver-embedded thread electrode with a 2.5 mm lens (Ocuscience, Rolla, MO, USA) was placed in contact with the central cornea. A 15 W red light was used to enable accurate electrode placement. This maneuver did not affect dark adaptation, and was switched off during recordings. ERG a-wave, and b-wave, pSTR, and PhNR were assessed using HMsERG software version 3.6 (Ocuscience, Rolla, MO, USA). To assess scotopic ERG a-wave and b-wave, responses to 15 full-field flashes separated by a 10 s interval (flash intensity 10 cd.s.m^{-2}) were averaged. For pSTR recording, responses to 10 full-field flashes separated by a 10 s interval (flash intensity 3.10^{-5} cd.s.m^{-2}) were averaged. Finally, after light adaptation (30 cd.s.m^{-2} for 10 min), responses from a photopic series (0.01—25 cd.s.m^{-2}, 32 flashes per intensity) were recorded, and PhNR recordings at 25 cd.s.m^{-2} were averaged.

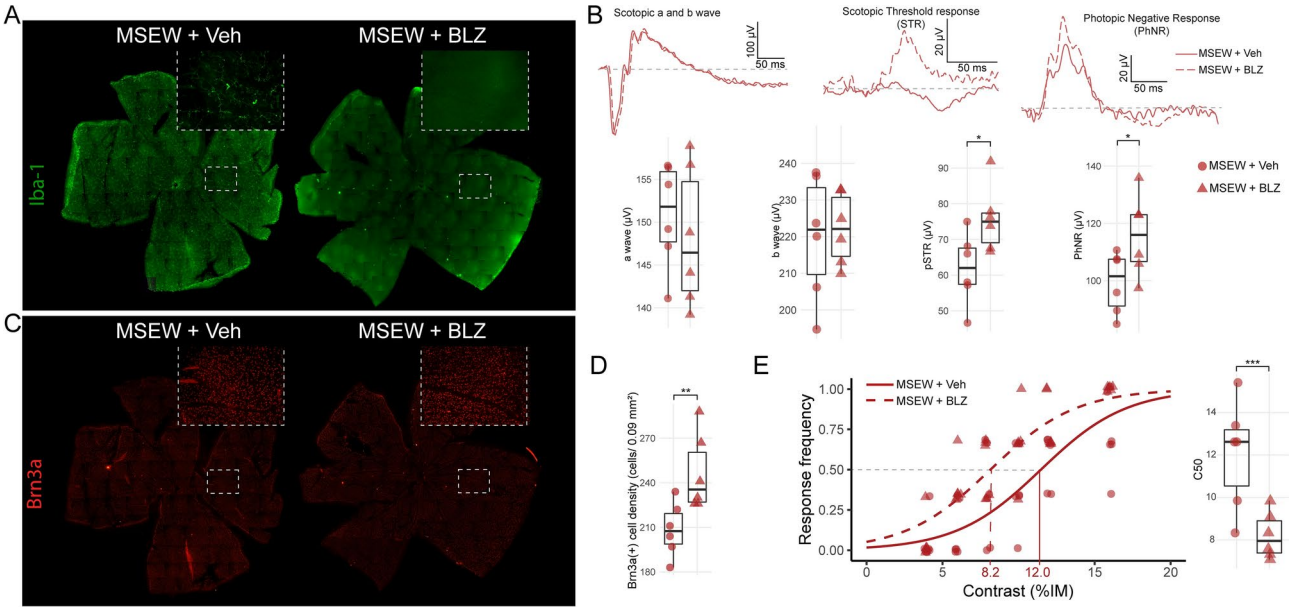

Fig. 7. Effect of BLZ945 treatment in MSEW mice. **A**. Representative images of Iba-1-immunoreactivity in the inner retina. BLZ945 treatment from PND 35 to PND 60 depleted retinal microglial cells in early stressed mice. **B**. BLZ945 did not change ERG a-wave or b-wave amplitudes, but significantly improved pSTR and PhNR amplitudes. **C**. Representative images of Brn3a-immunoreactivity. **D**. BLZ945 preserved Brn3a (+) RGC number in MSEW mice. **E**. In MSEW animals, BLZ945 induced a leftward shift in LTCV curves, as compared to early stressed animals receiving vehicle. ANOVA and Tukey post hoc tests were conducted. Significance levels: *P < 0.05, ** P < 0.01, *** P < 0.001, n = 6 litters/group.

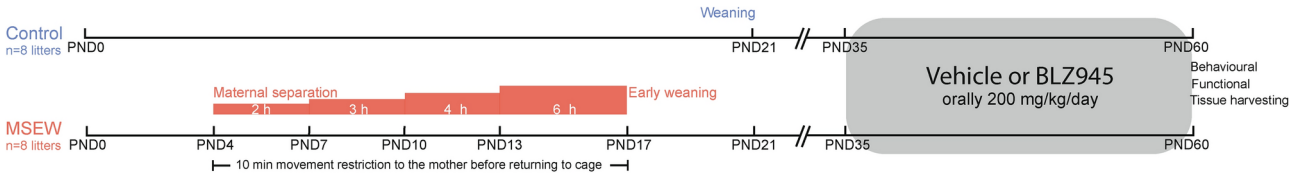

Fig. 8. Experimental protocols. MSEW pups were separated from their mothers from PND 4 to PND 17. Before returning with the dam, mothers were subjected to movement restriction for 10 min. A group of control of MSEW animals received vehicle or 200 mg/kg/day BLZ945 orally from PND 35 to PND 60. Functional studies and tissue harvesting were performed at PND 35, 45 or 60, and behavioral tests were performed at PND 60.

Immunohistochemical studies

Animals from different litters were anesthetized and intracardially perfused. Eyeballs were carefully removed, immersed for 24 h in a fixative solution; corneas and lens were removed, and whole-mount retinas were obtained and oriented. Then, retinas were immersed in 0.1 mol/L PBS, containing 0.1% Triton X-100 for 20 min, incubated overnight with 0.2% equine serum in PBS for unspecific blockade, and primary antibodies were added (Table 1). After several washes, retinas were incubated with a donkey anti-goat secondary antibody conjugated to Alexa 568, and/or a donkey anti-rabbit secondary antibody conjugated to Alexa 488 (Table 1) for 2 h at room temperature. Nuclei were stained with Hoechst (1 µg/ml, Sigma Chemical Co., St Louis, MO, USA). Finally, retinas were mounted with fluorescent mounting medium (Dako, Roche Biocare, Buenos Aires, Argentina). To determine RGC number, retinas were incubated with an anti-Brn3a antibody (Table 1), and observed under an epifluorescence microscope (BX50; Olympus, Tokyo, Japan), equipped with a 20 × lens and connected to a video camera (3 CCD; Sony, Tokyo, Japan), attached to a computer running image analysis software (Image-Pro Plus; Media Cybernetics Inc., Bethesda, MD, USA). The number of Brn3a (+) RGC were manually quantified under masked conditions with Fiji software in four 150 µm^2-sections, and averaged. For microglial morphometric analysis in the inner retina, retinas were incubated with an anti-Brn3a and an anti-Iba-1 antibody. Confocal z-stacks (1 µm step size) were taken using a Leica TCS SPE microscope equipped with a 40 × lens. Since MSEW did not affect microglial cells in the outer retina[24], only Iba-1 (+) cells from the inner retina were analyzed. For this purpose, Iba-1 (+) cells were analyzed only in those stacks in which Brn3a (+) RGC were present. To analyze microglial morphometric parameters, images were converted to binary images after a custom threshold procedure. For Sholl analysis, individual Iba-1 (+) cells were analyzed using Fiji SNT plugin[64]. For pro-

Target	Host	Dilution	Manufacturer	Research Resource Identifiers (RRID)
Brn3a	Goat	1/500	Santa Cruz Biotechnology	AB_2167511
Iba-1	Rabbit	1/1000	Wako Pure Chemical Industries	AB_839504
p-65	Mouse	1/200	Santa Cruz Biotechnology	AB_628017
C3	Mouse	1/200	Santa Cruz Biotechnology	AB_627277
NOS-2	Mouse	1/200	Santa Cruz Biotechnology	AB_627810
IL-1β	Mouse	1/200	Santa Cruz Biotechnology	AB_627791
Goat IgG	Donkey	1/500	Invitrogen Molecular Probes	AB_2534102
Rabbit IgG	Donkey	1/500	Invitrogen Molecular Probes	AB_2534017
Mouse IgG	Donkey	1/500	Invitrogen Molecular Probes	AB_141607

Table 1. Targets, hosts, dilutions, manufacturers, and RRID for antibodies used in immunohistochemical studies.

inflammatory marker analysis in microglial cells, flat-mounted retinas were co-incubated with Iba-1 and either p-65, C3, NOS-2 or IL-1β antibodies. Three 1 µm stacks were used to reconstruct microglial cells from z-stacks. To quantify p-65 positive nuclei, a binary mask was constructed using Hoechst channel, and p-65 intensity was analyzed within Hoechst positive area. Only those nuclei from Iba-1 (+) cells were analyzed. A positivity threshold was arbitrarily chosen for p65(+) nuclei. To quantify C3-, NOS-2-, and IL-1β-immunoreactivity at Iba-1 (+) cells, a binary mask was constructed using the Iba-1 channel, and pro-inflammatory markers intensity was measured only in Iba-1 (+) positive area.

Looming test with disk/background contrast variations

Responses to the LTCV were obtained as previously described[60]. Briefly, animals were habituated to the experimental room for 2 h, without food or water restrictions. Animals were gently placed in the looming arena, and allowed to acclimate for 5 min before the first stimulus presentation. Mice were presented with a dark expanding disk on different grey background levels in a random fashion. The disk/background contrast level was assessed by measuring the irradiance, using a photometer positioned at the center of the arena, as previously described[60].

$$MI(\%) = (Id - Ib)*100/(Id + Ib).$$

A range of contrasts was constructed between the lowest contrast that did not provoke response in any control animal, and the highest contrast that, consistently, elicited response in all control animals. Particularly, five different black disk/grey background contrasts were used for these experiments, each repeated three times, resulting in 15 individual looming stimuli, randomly presented for each animal. Each experimental session was recorded with a video camera for later analysis, and each stimulus was manually triggered by an operator only when the animal was near to the center of the arena. To evaluate the relationship between stimulus contrast and response, the proportion of positive responses (including all stereotyped responses: running, freezing, and upward rearing) was measured for each contrast. The frequency of response was calculated as the ratio of positive responses versus total stimuli applied for each contrast in each animal. The influence of contrast magnitude and experimental group on the probability of eliciting a defensive response was assessed using a binomial generalized linear model (GLM) with a logit link function. The logit link function is bounded between 0 and 1, and the binomial distribution is typically used to model probability data. For behavioral analysis, video recordings of experimental sessions were analyzed using DeepLabCut[65] to assess locomotor activity (distance traveled and velocity) during the acclimatization period. Response to the looming stimuli were analyzed by three independent masked observers. The disk/background contrast necessary to elicit a 50% positive response ("C50") for each animal was predicted using the corresponding GLM[60].

Data analysis

Experimenters were blinded to group assignment and outcomes for all experiments. No sample size calculation was performed. Normality was assessed by Shapiro Wilks test, and no tests were performed to detect outliers. The statistical analysis was performed using R statistical software, "lme4" package was used for linear mixed models. Groups (control or MSEW), treatments (vehicle or BLZ945) and sex, were used as fixed effects. No cases were found in which sex explained significant variance differences. Litter was used as a random effect. For ERG recordings in which both eyes from an animal were recorded, and for quantification of Iba-1 (+) cells related parameters, in which more than one cell from the same animal was analyzed, the individual was also used as a random effect. Statistical analysis was made by two- or three-way analysis of variance (ANOVA), and if an overall significant difference was detected, Tukey's HSD post-hoc test was carried out. Significance was set at P values below 0.05 for all analyses.

Data availability

The data sets used and/or analyzed during the current study are available from the corresponding author on reasonable request.

Received: 13 September 2024; Accepted: 6 May 2025

Published online: 17 May 2025

References

1. Danese, A. et al. Adverse childhood experiences and adult risk factors for age-related disease. *Arch. Pediatr. Adolesc. Med.* **163**, 1135–1143 (2009).
2. Hedges, D. W. & Woon, F. L. Early-life stress and cognitive outcome. *Psychopharmacology* **214**, 121–130 (2011).
3. Dalmasso, C. et al. Female mice exposed to postnatal neglect display angiotensin II–dependent obesity-induced hypertension. *J. Am. Heart Assoc.* **8**, e012309 (2019).
4. Felitti, V. J. et al. Relationship of childhood abuse and household dysfunction to many of the leading causes of death in adults. *Am. J. Prev. Med.* **14**, 245–258 (1998).
5. Gilbert, L. K. et al. Childhood adversity and adult chronic disease. *Am. J. Prev. Med.* **48**, 345–349 (2015).
6. Irish, L., Kobayashi, I. & Delahanty, D. L. Long-term physical health consequences of childhood sexual abuse: A meta-analytic review. *J. Pediatr. Psychol.* **35**, 450–461 (2010).
7. Spinhoven, P. et al. The specificity of childhood adversities and negative life events across the life span to anxiety and depressive disorders. *J. Affect. Disord.* **126**, 103–112 (2010).
8. Springer, K. W., Sheridan, J., Kuo, D. & Carnes, M. Long-term physical and mental health consequences of childhood physical abuse: Results from a large population-based sample of men and women. *Child Abuse Negl.* **31**, 517–530 (2007).
9. Wegman, H. L. & Stetler, C. A meta-analytic review of the effects of childhood abuse on medical outcomes in adulthood. *Psychosom. Med.* **71**, 805–812 (2009).
10. Afifi, T. O. et al. Population attributable fractions of psychiatric disorders and suicide ideation and attempts associated with adverse childhood experiences. *Am. J. Public Health* **98**, 946–952 (2008).
11. Bian, Y. et al. Prolonged maternal separation induces the depression-like behavior susceptibility to chronic unpredictable mild stress exposure in mice. *Biomed. Res. Int.* **2021**, 1–11 (2021).
12. Nishi, M., Horii-Hayashi, N. & Sasagawa, T. Effects of early life adverse experiences on the brain: implications from maternal separation models in rodents. *Front. Neurosci.* **8**, 166 (2014).
13. Nishi, M. Effects of early-life stress on the brain and behaviors: Implications of early maternal separation in rodents. *Int. J. Mol. Sci.* **21**, 7212 (2020).
14. Čater, M. & Majdič, G. How early maternal deprivation changes the brain and behavior?. *Eur. J. Neurosci.* **55**, 2058–2075 (2022).
15. Carlyle, B. C. et al. Maternal separation with early weaning: A rodent model providing novel insights into neglect associated developmental deficits. *Dev. Psychopathol.* **24**, 1401–1416 (2012).
16. George, E. D., Bordner, K. A., Elwafi, H. M. & Simen, A. A. Maternal separation with early weaning: a novel mouse model of early life neglect. *BMC Neurosci.* **11**, 123 (2010).
17. Gracia-Rubio, I. et al. Maternal separation induces neuroinflammation and long-lasting emotional alterations in mice. *Prog. Neuropsychopharmacol. Biol. Psych.* **65**, 104–117 (2016).
18. Aleksić, D. et al. Long-term effects of maternal deprivation on the volume, number and size of neurons in the amygdala and nucleus accumbens of rats. *Psychiatr. Danub.* **28**, 211–219 (2016).
19. de Azeredo, L. A. et al. Maternal separation induces hippocampal changes in cadherin-1 (CDH-1) mRNA and recognition memory impairment in adolescent mice. *Neurobiol. Learn. Mem.* **141**, 157–167 (2017).
20. Orso, R. et al. A systematic review and multilevel meta-analysis of the prenatal and early life stress effects on rodent microglia, astrocyte, and oligodendrocyte density and morphology. *Neurosci. Biobehav. Rev.* **150**, 105202 (2023).
21. Tomoda, A. et al. Reduced prefrontal cortical gray matter volume in young adults exposed to harsh corporal punishment. *Neuroimage* **47**, T66–T71 (2009).
22. Gold, A. L. et al. Childhood abuse and reduced cortical thickness in brain regions involved in emotional processing. *J. Child Psychol. Psych.* **57**, 1154–1164 (2016).
23. Yao, A. et al. Subclinical structural atypicality of retinal thickness and its association with gray matter volume in the visual cortex of maltreated children. *Sci. Rep.* **14**, 11465 (2024).
24. Calanni, J. S. et al. Early life stress induces visual dysfunction and retinal structural alterations in adult mice. *J. Neurochem.* **165**, 362–378 (2023).
25. de Pablos, R. M. et al. Chronic stress enhances microglia activation and exacerbates death of nigral dopaminergic neurons under conditions of inflammation. *J. Neuroinflammation* **11**, 34 (2014).
26. Jauregui-Huerta, F. et al. Responses of glial cells to stress and glucocorticoids. *Curr. Immunol. Rev.* **6**, 195–204 (2010).
27. Grigoruta, M. et al. Maternal separation induces retinal and peripheral blood mononuclear cell alterations across the lifespan of female rats. *Brain Res.* **1749**, 147117 (2020).
28. Allen, N. J. & Lyons, D. A. Glia as architects of central nervous system formation and function. *Science* **1979**(362), 181–185 (2018).
29. Chitu, V. & Stanley, E. R. Regulation of embryonic and postnatal development by the CSF-1 receptor. *Curr. Top. Dev. Biol.* **123**, 229–275 (2017).
30. Elmore, M. R. P. et al. Colony-stimulating factor 1 receptor signaling is necessary for microglia viability, unmasking a microglia progenitor cell in the adult brain. *Neuron* **82**, 380–397 (2014).
31. Chitu, V. et al. Emerging roles for CSF-1 receptor and its ligands in the nervous system. *Trends Neurosci.* **39**, 378–393 (2016).
32. Reemst, K. et al. Early-life stress lastingly impacts microglial transcriptome and function under basal and immune-challenged conditions. *Transl. Psych.* **12**, 507 (2022).
33. Sequeira, M. K. & Bolton, J. L. Stressed microglia: Neuroendocrine-neuroimmune interactions in the stress response. *Endocrinology* **164**, bqad088 (2023).
34. Ozdamar Unal, G. et al. The effect of Vortioxetine on the NLRP3 pathway and microglial activity in the prefrontal cortex in an experimental model of depression. *Immunopharmacol. Immunotoxicol.* **46**, 264–275 (2024).
35. Catale, C., Gironda, S., Lo Iacono, L. & Carola, V. Microglial function in the effects of early-life stress on brain and behavioral development. *J. Clin. Med.* **9**, 468 (2020).
36. Cattane, N. et al. Preclinical animal models of mental illnesses to translate findings from the bench to the bedside: Molecular brain mechanisms and peripheral biomarkers associated to early life stress or immune challenges. *Eur. Neuropsychopharmacol.* **58**, 55–79 (2022).
37. Deng, S. et al. Early-life stress contributes to depression-like behaviors in a two-hit mouse model. *Behav. Brain Res.* **452**, 114563 (2023).
38. Gildawie, K. R., Orso, R., Peterzell, S., Thompson, V. & Brenhouse, H. C. Sex differences in prefrontal cortex microglia morphology: Impact of a two-hit model of adversity throughout development. *Neurosci. Lett.* **738**, 135381 (2020).
39. Dutcher, E. G. et al. Early-life stress biases responding to negative feedback and increases amygdala volume and vulnerability to later-life stress. *Transl. Psych.* **13**, 81 (2023).
40. Zhang, Y. D., Shi, D.-D., Zhang, S. & Wang, Z. Sex-specific transcriptional signatures in the medial prefrontal cortex underlying sexually dimorphic behavioural responses to stress in rats. *J. Psych. Neurosci.* **48**, E61–E73 (2023).
41. Bachiller, S., Paulus, A., Vázquez-Reyes, S., García-Domínguez, I. & Deierborg, T. Maternal separation leads to regional hippocampal microglial activation and alters the behavior in the adolescence in a sex-specific manner. *Brain Behav. Immun. Health* **9**, 100142 (2020).

42. del Fernández-Arjona, M. et al. Microglial morphometric parameters correlate with the expression level of IL-1β, and allow identifying different activated morphotypes. *Front. Cell. Neurosci.* https://doi.org/10.3389/fncel.2019.00472 (2019).
43. Panda, S. P., Reddy, P. H., Gorla, U. S. & Prasanth, D. Neuroinflammation and neovascularization in diabetic eye diseases (DEDs): Identification of potential pharmacotherapeutic targets. *Mol. Biol. Rep.* **50**, 1857–1869 (2023).
44. Sato, K. et al. CHOP deletion and anti-neuroinflammation treatment with hesperidin synergistically attenuate NMDA retinal injury in mice. *Exp. Eye Res.* **213**, 108826 (2021).
45. Tang, F. et al. The expression and role of PIDD in retina after optic nerve crush. *J. Mol. Histol.* **51**, 89–97 (2020).
46. Wang, A. L., Yu, A. C. H., He, Q. H., Zhu, X. & Tso, M. O. M. AGEs mediated expression and secretion of TNF alpha in rat retinal microglia. *Exp. Eye Res.* **84**, 905–913 (2007).
47. Harder, J. M. et al. Early immune responses are independent of RGC dysfunction in glaucoma with complement component C3 being protective. *Proc. Natl. Acad. Sci.* **114**, E3839–E3848 (2017).
48. Luo, C., Zhao, J., Madden, A., Chen, M. & Xu, H. Complement expression in retinal pigment epithelial cells is modulated by activated macrophages. *Exp. Eye Res.* **112**, 93–101 (2013).
49. Kuehn, S. et al. Interaction of complement system and microglia activation in retina and optic nerve in a NMDA damage model. *Mol. Cell. Neurosci.* **89**, 95–106 (2018).
50. Rutar, M. et al. Analysis of complement expression in light-induced retinal degeneration: Synthesis and deposition of C3 by microglia/macrophages is associated with focal photoreceptor degeneration. *Invest. Opthalmol. Vis. Sci.* **52**, 5347 (2011).
51. Natoli, R. et al. Obesity-induced metabolic disturbance drives oxidative stress and complement activation in the retinal environment. *Mol. Vis.* **24**, 201–217 (2018).
52. Silverman, S. M., Ma, W., Wang, X., Zhao, L. & Wong, W. T. C3- and CR3-dependent microglial clearance protects photoreceptors in retinitis pigmentosa. *J. Exp. Med.* **216**, 1925–1943 (2019).
53. Catale, C. et al. Early life social stress causes sex- and region-dependent dopaminergic changes that are prevented by minocycline. *Mol. Neurobiol.* **59**, 3913–3932 (2022).
54. Bordone, M. P. et al. Involvement of microglia in early axoglial alterations of the optic nerve induced by experimental glaucoma. *J. Neurochem.* **142**, 323–337 (2017).
55. Song, Y. et al. Microglial repopulation restricts ocular inflammation and choroidal neovascularization in mice. *Front. Immunol.* https://doi.org/10.3389/fimmu.2024.1366841 (2024).
56. Cheng, X. et al. Repopulated retinal microglia promote Müller glia reprogramming and preserve visual function in retinal degenerative mice. *Theranostics* **13**, 1698–1715 (2023).
57. Laudenberg, N., Kinuthia, U. M. & Langmann, T. Microglia depletion/repopulation does not affect light-induced retinal degeneration in mice. *Front. Immunol.* **14**, 1345382 (2024).
58. Karg, M. M. et al. Microglia preserve visual function in the aging retina by supporting retinal pigment epithelial health. *Immun. Ageing* **20**, 53 (2023).
59. He, J. et al. Disease-associated microglial activation prevents photoreceptor degeneration by suppressing the accumulation of cell debris and neutrophils in degenerating rat retinas. *Theranostics* **12**, 2687–2706 (2022).
60. Calanni, J. S. et al. An ethologically relevant paradigm to assess defensive response to looming visual contrast stimuli. *Sci. Rep.* **14**, 12499 (2024).
61. Alex, A. M. et al. A global multicohort study to map subcortical brain development and cognition in infancy and early childhood. *Nat. Neurosci.* **27**, 176–186 (2024).
62. Wies Mancini, V. S. B., Pasquini, J. M., Correale, J. D. & Pasquini, L. A. Microglial modulation through colony-stimulating factor-1 receptor inhibition attenuates demyelination. *Glia* **67**, 291–308 (2019).
63. Dieguez, H. H. et al. Superior cervical gangliectomy induces non-exudative age-related macular degeneration in mice. *Dis. Model Mech.* https://doi.org/10.1242/dmm.031641 (2018).
64. Ferreira, T. A. et al. Neuronal morphometry directly from bitmap images. *Nat. Methods* **11**, 982–984 (2014).
65. Mathis, A. et al. DeepLabCut: Markerless pose estimation of user-defined body parts with deep learning. *Nat. Neurosci.* **21**, 1281–1289 (2018).

Acknowledgements

This research was supported by grants from the Agencia Nacional de Promoción Científica y Tecnológica [PICT 0415]; The University of Buenos Aires [20020170100392BA]; Consejo Nacional de Investigaciones Científicas y Técnicas [PIP 0630], Argentina. The authors declare that they have no known competing financial interests or personal relationships that could have appeared to influence the work reported in this paper.

Author contributions

JSC planned and performed experiments, formal analysis, and conceived the whole project; LAP provided scientific guidance, support with techniques, conceptualization, and edited the manuscript. HHD, NBA, and BB performed experiments. DD formal analysis, conceptualization, critically evaluated and edited the manuscript. RER conceived, supervised the whole project, and drafted the manuscript.

Funding

Agencia Nacional de Promoción de la Investigación, el Desarrollo Tecnológico y la Innovación, PICT 0415, Universidad de Buenos Aires, 20020170100392BA, Consejo Nacional de Investigaciones Científicas y Técnicas, PIP 0630.

Declaration

Competing interests

The authors declare no competing interests.

Additional information

Supplementary Information The online version contains supplementary material available at https://doi.org/10.1038/s41598-025-01526-w.

Correspondence and requests for materials should be addressed to R.E.R.